Appl Phys A (2012) 109:835–840
DOI 10.1007/s00339-012-7390-8

**Applied Physics A**
**Materials Science & Processing**

# Enhancing coherent nonlinear-optical processes in nonmagnetic backward-wave materials

**Alexander K. Popov · Mikhail I. Shalaev · Sergey A. Myslivets · Vitaly V. Slabko · Igor S. Nefedov**

Received: 16 November 2011 / Accepted: 10 October 2012 / Published online: 7 November 2012


**Abstract** Novel concepts of nonlinear-optical (NLO) photonic metamaterials (MMs) are proposed. They concern with greatly enhanced coherent NLO energy exchange between ordinary and backward waves (BWs) through the frequency-conversion processes. Two different classes of materials which support BWs are considered: crystals that support optical phonons with negative group velocity and MMs with specially engineered spatial dispersion. The possibility to replace plasmonic NLO MMs enabling magnetic response at optical frequencies, which are very challenging to engineer, by the ordinary readily available crystals, are discussed. The possibility to mimic extraordinary NLO frequency-conversion propagation processes attributed to negative-index MMs (NIMs) is shown in some of such crystals, if optical phonons with negative group velocity and a proper phase-matching geometry are implemented. Here, optical phonons are used as one of the coupled counterparts instead of backward electromagnetic waves (BEMWs). The appearance of BEMWs in metaslabs made of carbon nanotubes, the possibilities and extraordinary properties of BW second harmonic generation in such MMs is another option of nonmagnetic NIMs, which is described too. Among the applications of the proposed photonic materials is the possibility of creation of a family of unique BW photonic devices such as frequency doubling metamirror and Raman amplifiers with greatly improved efficiency.

A.K. Popov (✉)
University of Wisconsin-Stevens Point, Stevens Point, WI 54481, USA
e-mail: apopov@uwsp.edu

M.I. Shalaev · V.V. Slabko
Siberian Federal University, 660041 Krasnoyarsk, Russian Federation

S.A. Myslivets
Institute of Physics of Russian Academy of Sciences, 660036 Krasnoyarsk, Russian Federation

I.S. Nefedov
SMARAD Center of Excellence, Aalto University, 00076 Aalto, Finland

## 1 Introduction

Optical NIMs form a novel class of electromagnetic media that promises revolutionary breakthroughs in photonics. The possibilities of such breakthroughs originate from backwardness, the extraordinary property that electromagnetic waves acquire in NIMs. Unlike ordinary, positive-index materials, the energy flow **S** and the wave-vector **k** are counter-directed in NIMs. This determines their unique linear and NLO propagation properties. Usually, NIMs are nanostructured metal–insulator composites comprised of the nanoscopic metal resonators that enable magnetic response at optical frequencies. Extraordinary features of coherent NLO energy conversion processes in NIMs that stem from wave-mixing of ordinary and backward EMWs, and the possibilities to apply them for compensating the outlined losses have been reviewed [1, 2]. A remarkable feature is distributed feedback behavior which allows for sharp resonance concentration of generated fields in a microscopic zones and great increase of the conversion efficiency. Essentially different properties of three-wave mixing (TWM) and second harmonic generation (SHG) have been shown.

While the physics and applications of NIMs are being explored worldwide at a rapid pace, current mainstream focuses on fabrication of specially shaped nanostructures which enable negative optical magnetism. It is a challenging task that relies on sophisticated methods of nanotechnology. Engineering of a strong fast quadratic and cubic

NLO response by such mesoatoms also presents a challenging goal not yet achieved. This paper considers alternative possibilities to advance the state of the art of the nonlinear photonic materials through the development of novel paradigms for quantum engineering of coherent nonlinear NIMs. Two approaches are discussed. One grounds itself on replacing one of the coupled EM waves by the negative-dispersive phonons, which is possible by making use of readily available dielectric crystals. The other option considers metamaterials where backwardness of one of the coupled propagating EM waves originates from deliberately engineered spatial dispersion of the nanoscopic metamaterial building blocks. None of such constituents itself must possess nanoresonator properties providing negative optical magnetism.

## 2 Enhancing coherent energy transfer between electromagnetic waves through backward optical phonons

Extraordinary features of coherent NLO energy conversion processes in NIM that stem from wave-mixing of ordinary and backward EMWs, and the possibilities to apply them for compensating the outlined losses have been shown [6–15]. Essentially different properties of three-wave mixing (TWM) and four-wave mixing (FWM) processes on the one hand and second harmonic (SHG) and third harmonic generation (THG) on the other have been revealed [1–6, 16–18]. Ultimately, NLO with BW enables a great enhancement of energy-conversion rate at the otherwise equal nonlinearities and intensities of input waves. Herein, we propose fundamentally different scheme of TWM of ordinary and backward waves (BWs). It builds on the stimulated Raman scattering (SRS) where two ordinary EM waves excite backward elastic vibrational wave in a crystal, which results in TWM. The possibility of such BWs was predicted by L.I. Mandelstam in 1945 [19], who also had pointed out that negative refraction is a general property of the BWs. The idea underlying the proposed concept and its basic justification is described below (see also [20]). The goal is to show the possibility to replace the NI plasmonic composites, which are challenging to fabricate, with readily available ordinary crystals, some of which have been already extensively studied, and thus to mimic the unparallel properties of coherent NLO energy exchange between the ordinary and backward waves.

The basic idea is as follows. The dispersion curve $\omega(k)$ of phonons in the crystals containing more than one atom per unit cell has two branches: acoustic and optical. For the optical branch, the dispersion is negative in the range from zero to the boundary of the first Brillouin zone (Fig. 1). Hence, the group velocity of optical phonons, $\mathbf{v}_v^{\rm gr}$, is antiparallel

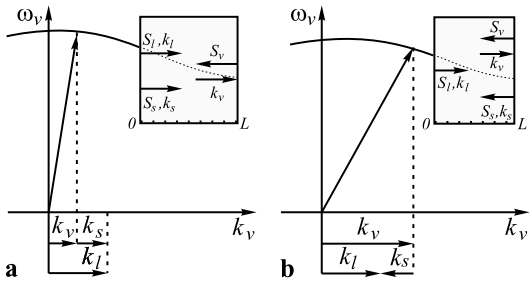


**Fig. 1** Negative dispersion of optical phonons and two phase matching options for short- and long-wave vibrations: (**a**) co-propagating, (**b**) contra-propagating fundamental (control) and Stokes (signal) waves. *Insets*: relative directions of the energy flows and the wave-vectors

with respect to its wave-vector, $\mathbf{k}_v^{\rm ph}$, and phase velocity, $\mathbf{v}_v^{\rm ph}$, because

$$\mathbf{S} = \mathbf{v}_g U, \quad \mathbf{v}_g = (\mathbf{k}/k)[\partial\omega/\partial k], \ \partial\omega(k)/\partial k < 0. \tag{1}$$

Optical vibrations can be excited by the light waves due to the two-photon (Raman) scattering. The latter gives the ground to consider such a crystal as the analog of the medium with negative refractive index at the phonon frequency and to examine the processes of parametric interaction of three waves, two of which are ordinary EM waves and the third is the wave of elastic vibrations with the directions of the energy flow and of the wave-vector opposite to each other. Here, we will consider only lowest-order Raman process [21, 22]. The waves are given by the equations

$$E_{l,s} = (1/2)\varepsilon_{l,s}(z,t)e^{ik_{l,s}z - i\omega_{l,s}t} + \text{c.c.}, \tag{2}$$

$$Q_v = (1/2)Q(z,t)e^{ik_v z - i\omega_v t} + \text{c.c.} \tag{3}$$

Here, $\varepsilon_{l,s}$, $Q$, $\omega_{l,s,v}$ and $k_{l,s,v}$ are the amplitudes, frequencies and wave-vectors of the fundamental, Stokes and vibrational waves; $Q_v(z,t) = \sqrt{\rho}x(z,t)$, with $x$ the displacement of the vibrating particles and $\rho$ the medium density. With account for the energy and momentum conservation,

$$\omega_l = \omega_s + \omega_v(k_v), \qquad \vec{k}_l = \vec{k}_s(\omega_s) + \vec{k}_v,$$

one obtains the following equations for the slowly varying amplitudes in the approximation of the of first order of $Q$ in the polarization expansion:

$$\frac{\partial\varepsilon_l}{\partial z} + \frac{1}{v_l^{\rm gr}}\frac{\partial\varepsilon_l}{\partial t} = i\frac{\pi\omega_l^2}{k_l c^2}N\frac{\partial\alpha}{\partial Q}\varepsilon_s Q, \tag{4}$$

$$\frac{\partial\varepsilon_s}{\partial z} + \frac{1}{v_s^{\rm gr}}\frac{\partial\varepsilon_s}{\partial t} = i\frac{\pi\omega_s^2}{k_s c^2}N\frac{\partial\alpha}{\partial Q}\varepsilon_l Q^*, \tag{5}$$

$$\frac{\partial Q}{\partial z} + \frac{1}{v_v^{\rm gr}}\frac{\partial Q}{\partial t} + \frac{Q}{\tau v_v^{\rm gr}} = i\frac{1}{4\omega_v v_v^{\rm gr}}N\frac{\partial\alpha}{\partial Q}\varepsilon_l\varepsilon_s^*. \tag{6}$$

Here, $v_{l,s,v}^{\rm gr}$ are the projections of the group velocities of the fundamental, Stokes and vibration waves on the $z$-axis; $N$ is the number density of the vibrating molecules; $\alpha$ is the molecule polarizability; $\tau$ is phonon lifetime; and $\omega_0$ is

phonon frequency for $k_v = 0$. The dispersion $\omega_v(k_v)$ can be approximated as $\omega_v = \sqrt{\omega_0^2 - \beta k_v^2}$ (see [21]). Then, in the vicinity of $k_v = 0$, velocity $v_v^{\rm gr}$ is given by $v_v^{\rm gr} = -\beta k_v/\omega_v = -\beta/v_v^{\rm ph}$, where $v_v^{\rm ph}$ is the projection of the phase velocity of the vibrational wave on the $z$-axis and $\beta$ is the dispersion parameter for the given crystal.

For the sake of clarity, the continuous wave case and the approximation of the constant field $E_l$ is considered. The latter is appropriate for the relatively week Stokes and vibrational waves. Then (5) and (6) take the form

$$dQ/dz = -ig_1\varepsilon_s^* - Q/\big(\tau v_v^{\rm gr}\big), \qquad d\varepsilon_s/dz = ig_2 Q^*. \quad (7)$$

Here,

$$g_1 = -N(\partial\alpha/\partial Q)\varepsilon_l/\big(4\omega_v v_v^{\rm gr}\big), \quad (8)$$

$$g_2 = \big(\pi\omega_s^2/k_s c^2\big)N(\partial\alpha/\partial Q)\varepsilon_l. \quad (9)$$

In the case of Fig. 1(a), (7) exhibit *three fundamental differences* as compared with TWM of co-propagating waves in ordinary materials: an opposite sign with $g_1$ which stems from $v_v^{\rm gr} < 0$, an opposite sign with $Q/(\tau v_v^{\rm gr})$ because the phonon flow is against the $z$-axis, and the boundary conditions for $Q$ to be defined at $z = L$, i.e. at the opposite edge of the slab as compared to that for $\varepsilon_s$. This leads to *fundamental changes* in their solutions and, consequently, in the spatial and output behavior of the Stokes signal. Alternatively, in the given constant $\varepsilon_l$ approximation, the equations become identical and the behavior standard for the case of Fig. 1(b). The solution to (7) is found in the form

$$Q^* = A_1 e^{\beta_1 z'} + A_2 e^{\beta_2 z'}, \qquad \varepsilon_s = A_3 e^{\beta_1 z'} + A_4 e^{\beta_2 z'}, \quad (10)$$

where $\beta_{1,2} = 1 \mp iR$ with $R = \sqrt{g_1^* g_2 l_p^2 - 1}$; $z' = z/l_p$, $l_p = -2v_v^{\rm gr}\tau$. The amplitudes $A_{1-4}$ and their relationships are determined by the boundary conditions. Transmission factors for co-propagating, $T_s^{\uparrow\uparrow}(z)$, and counter-propagating ($g_2 < 0$), $T_s^{\uparrow\downarrow}(z)$, fundamental and Stokes waves are found as

$$T_s^{\uparrow\uparrow} = \left|\frac{e^{z'}\{R\cos[R(L'-z')] + \sin[R(L'-z')]\}}{R\cos(RL') + \sin(RL')}\right|^2, \quad (11)$$

$$T_s^{\uparrow\downarrow} = \left|\left\{\beta_1 e^{[\beta_2(L'-z')]} - \beta_2 e^{[\beta_1(L'-z')]}\right\}/2R\right|^2, \quad (12)$$

where $L' = L/l_p$, $T_s^{\uparrow\uparrow} = |\varepsilon_s(z)/\varepsilon_s(z=0)|^2$ and $T_s^{\uparrow\downarrow} = |\varepsilon_s(z)/\varepsilon_s(z=L)|^2$.

Equations (11) and (12) display spatial distributions which are *controlled* by the field $\varepsilon_l$ and are in a strict contrast to each other. It is explicitly seen for the ultimate loss-free case ($l_p \to \infty$). Then

$$T_s^{\uparrow\uparrow}(z=L) \to 1/\cos^2(gL), \quad (13)$$

$$T_s^{\uparrow\downarrow}(z=0) \to \big[\exp\big(2|g|L\big)\big]/4, \quad (14)$$

where $g = \sqrt{g_1^* g_2}$. Equation (11) depicts a series of sharp giant resonance enhancements of the output signal for $g \to (2j+1)\pi/2L$ ($j = 0, 1, 2, \ldots$). On the contrary, the coupling scheme of Fig. 1(b) is equivalent to scattering on acoustic phonons and on optical phonons with positive group velocity. Correspondingly, (12) displays typical exponential growth with no resonances with respect to intensity of the fundamental control field. In general case, the denominator in (11) can be turned to zero if $g^2 l_p^2 > 1$. The threshold value of intensity of the control field is $I_{\rm min} = (cn_s\lambda_{s0}\omega_v/8\pi^3 l_p\tau)|N\partial\alpha/\partial Q|^{-2}$, where $\lambda_{s0}$ is Stokes wavelength in the vacuum.

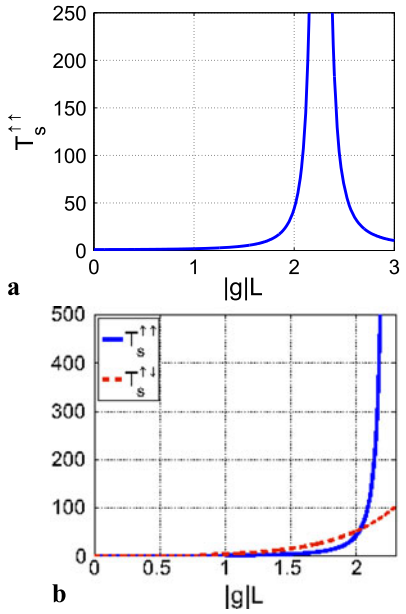


**Fig. 2** (**a**) Transmission of the Stokes wave $T_s^{\uparrow\uparrow}(z = L)$ vs. intensity of the fundamental control field in the vicinity of first "geometrical" resonance (co-propagating $E_l$ and $E_s$ geometry). Such extraordinary resonance appears because of backwardness of the coupled vibration wave. (**b**) Comparison of the output intensities of the Stokes wave vs. intensity of the control field for co-propagating (the *blue*, *solid line*) and contra-propagating (the *red*, *dashed line*) fundamental (control) and Stokes (signal) waves

For a given intensity of the control field $I_l > I_{\rm min}$, the crystal thickness corresponding to the first resonance is $L' = [\pi - \tan^{-1}(R)]/R$. Figure 2(a) depicts transmission in the vicinity of the first "geometrical" resonance. In the resonance, $T_s^{\uparrow\uparrow} \to \infty$, which is due to the approximation of constant control field. Conversion of the control field to the Stokes one and excited molecule vibrations would lead to saturation of the control field which limits the maximum achievable amplification. Strong amplification in the maximums indicates the possibility of self-oscillations and thus creation of *mirrorless* optical parametrical oscillator with unparalleled properties. In the case of Fig. 1(b), $k_s < 0$ and the denominator in (12) cannot be equal to zero. This results in exponential spatial dependence with no resonances depicted in Fig. 2(b) (the red, dashed line). Figure 2(b) shows that, in the vicinity of the resonance, three-wave coupling

of waves with co-directed wave-vectors and contra-directed energy flows of vibrational and Stokes waves provides for *much higher* efficiency of coherent energy conversion than in the standard schemes. Figure 2 indicates the possibility to *fit in* the effective conversion length within the crystal of a given thickness and to significantly *concentrate* the generated Stokes field nearby its output facet. Such atypical extraordinary behavior in readily available crystals may find exciting applications.

Such unusual properties are in a striking contrast with those attributed to commonly known counterparts, the crystals where only phonons with positive group velocity exist [21, 22]. Such NLO properties are also different from those inherent in the phase-matched mixing of EM and acoustic waves for the case where the latter has energy flux and wave-vector directed against EM waves [23]. The elaboration of the proposed concept will allow to utilize the revealed properties for creation of a family of unique photonic devices such as optical switches, filters, amplifiers and cavity-free optical parametric oscillators based on ordinary Raman crystals without the requirement of its periodical poling at the nanoscale (see[24] and references therein).

Estimations made for the model which is pertinent to the diamond crystal $\omega_v = 1332\ \mathrm{cm}^{-1}$ and the vibrational transition width $(c\tau)^{-1} = 1.56\ \mathrm{cm}^{-1}$ [25–27], have shown that the required excitation intensities are above the typical crystal breakdown threshold in the continuous wave regime. However, the cross section of the Raman scattering is inversely proportional to the squared frequency offset from the intermediate single-photon resonance. Therefore, the threshold intensity $I_{\min}$ can be reduced by seven to eight orders compared to its off-resonance values by approaching such a resonance. The breakdown threshold can be increased and required intensity reduced for pulsed lasers with the pulse length shorter than the phonon relaxation rate.

## 3 Backward waves, carbon nanoforest and second harmonic generation

Herewith, we suggest more general approach to generating backward *electromagnetic* waves, which is free from the limitations inherent to current mainstream approach. The latter relies on plasmonic nanoresonators which ensure negative optical magnetism. The basic idea is as follows. In a loss-free isotropic medium, energy flux $\mathbf{S}$ is directed along the group velocity $\mathbf{v}_g$:

$$\mathbf{S} = \mathbf{v}_g U, \quad \mathbf{v}_g = \mathrm{grad}_{\mathbf{k}}\omega(\mathbf{k}). \tag{15}$$

Here, $U$ is energy density attributed to EMW. It is seen that the group velocity may become directed *against* the wave-vector depending on sign of dispersion $\partial\omega/\partial k$. Similar property was discussed in the preceding section, however applied

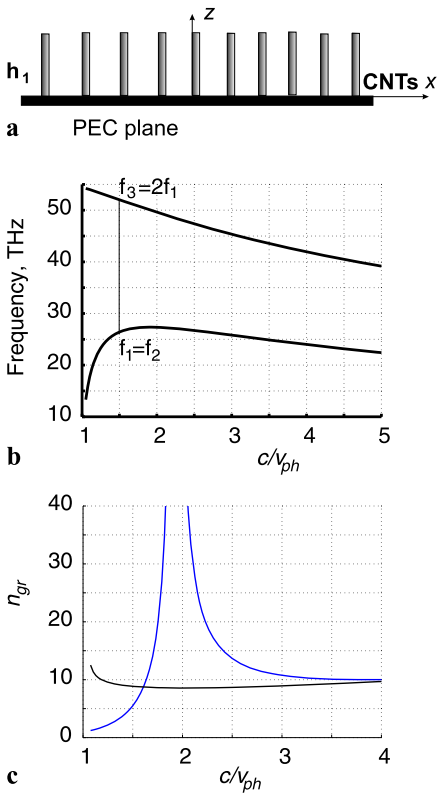


**Fig. 3** (**a**) Geometry of free-standing CNT. (**b**) Dispersion—the frequency vs. slow-wave factor for the slab of CNTs with open ends. (**c**) Group delay factor vs. the phase velocity slow-wave factor for the same modes as in panel (**a**). *Black* (*flat*) *curve* corresponds to the high-frequency mode, *blue curve* to the low-frequency mode. The tip of *blue curve* is cut. Its maximum corresponds to the stop-light regime

to *elastic* vibrational waves. Such an approach to engineering of BEMW discussed, e.g., in [28, 29] has not attracted significant research efforts so far. The search and elaboration of the particular MM with spatial dispersions that enables BEMW remains the topical problems of the day. Appearance of BEM modes in nanoarrays and layered structures has been shown recently [30, 31]. Obviously, many other options should exist. Each of them leaves open questions, both fundamental and specific to each potential material and application. Below, we propose and give a preliminary analysis pertinent to one such option that seems promising in the context of nonlinear propagation coherent energy conversion processes, such as generation of backward second harmonic.

Figure 3(a) depicts a periodic array of carbon nanotubes (CNT) vertically standing on the surface of a perfect electrical conductor (PEC) with the CNT ends open to air, which can be seen as perfect magnetic conductor (PMC). Such CNT arrays form finite-thickness slabs which have been fabricated by many research groups and used as field emitters, biosensors, antennas and in nanoelectronics. As shown in Ref. [32], EM waves traveling through such CNT "nanoforest," along $x$ or $y$ directions, possess a hyperbolic dispersion

and relatively low losses in the THz and mid-IR ranges. One of the most important consequences from the hyperbolic-type dispersion law is the possibility for propagation of both forward *and backward* EM waves. Consider EMW propagating along the $x$-axis. In such a one-dimensional case, (15) reads as $v_{\rm gr} = \partial\omega/\partial k_x$. We also introduce group $n_{\rm gr} = c/v_g$ and phase $n_{\rm ph} = c/v_{\rm ph}$ slow-wave factors. The latter one is a refractive index. For the given case of surface waves propagating in the slab of CNT with open ends, whose fields attenuate in air, the dispersion is given by the equation [33]:

$$\tan(k_z h) = \sqrt{k_x^2 - k^2}/k_z. \tag{16}$$

Such a dependence can be understood from considering a planar waveguide formed by perfect PEC and PMC planes and tampered with a CNT array. The array axis is orthogonal to the walls of the waveguide. Then, the propagation constant along the waveguide is given by

$$k_\perp = \sqrt{\epsilon_{zz}\left[k^2 - (m\pi/2h)^2\right]}, \tag{17}$$

where $m$ is a positive integer, $h$ is the height of the waveguide (CNT) and $k$ is the wavenumber in free space [34]. If $\epsilon_{zz} < 0$, BW propagation is allowed when $k < m\pi/2h$ and forbidden for $k > m\pi/2h$. The relation between the wave-vector component $k_x$ and wavenumber $k$ is

$$k_x^2 = \left[\left(k^2 - k_p^2\right)\left(k^2 - k_z^2\right)\right]/\left[k^2\right], \tag{18}$$

where $k_z = m\pi/(2h)$, $m$ is the integer determining a number of field variations along CNT, and $k_p$ is plasma wave-vector. One can show that $\mathrm{d}k_\perp^2/\mathrm{d}k^2 < 0$, if $k_z/k > 1$ and $k_p/k > 1$.

Numerical analysis of (16) is depicted in Fig. 3(b) for the case of CNT radius $r = 0.82$ nm, the lattice period $d = 15$ nm and EM modes with $m = 1$ and $m = 3$. The appearance of positive dispersion for small slow-wave factors is caused by interaction of BW in the CNT slab with the plane wave in air. Indeed, coexistence of the positive (ascending dependence) and negative (descending dependence) dispersion for different frequencies proves that such a metamaterial supports both ordinary and *backward* EMW. It also proves that resonant plasmonic structures, like split-ring resonators, exhibiting negative $\epsilon$ and $\mu$ are *not* the necessary requirement for the realization of BW regime in mid-IR range. The possibility of considerable increased bandwidth of BEMW compared to most plasmonic MM made of nanoscopic resonators which gives the ground to consider CNT arrays as a promising *perfect backward-wave metamaterial*. The slow-wave factor for both modes is shown in Fig. 3(c). The magnitude of $n_{\rm gr}$ goes to infinity at $n_{\rm ph} \approx 1.85$, which indicates the stop-light regime for the low-frequency mode. Particularly, Fig. 3(c, b) shows the possibility of *phase matched* SHG. The possibilities of independent quantum engineering of corresponding nonlinearities were shown in Refs. [1, 11, 13–15]. The attractive feature of given approach is the feasibility of tailoring the outlined properties.

## 4 Conclusions

While the physics and applications of NIM are being explored worldwide at a rapid pace, current mainstream focuses on fabrication of specially shaped nanostructures which enable negative optical magnetism. It is challenging task that relies on sophisticated methods of nanotechnology. Engineering a strong fast quadratic and cubic NLO response by such mesoatoms also presents a challenging goal not yet achieved. This paper proposes to advance the state-of-the-art of the nonlinear photonic materials through development of novel paradigms for enhanced coherent nonlinear coupling of EMW which is accompanied by efficient frequency conversion. Such an approach has become achievable only recently owing to fast developments in the fundamental electromagnetics, nanophotonics and in nanotechnology. It also paves the way to realization of exotic coherent NLO processes in some of readily available crystals. Among the potential applications are microscopic frequency-doubling nonlinear-optical mirrors and sensors, all-optical switching elements, frequency mixers, filters, amplifiers, and sources of entangled counter-propagating photons.

**Acknowledgement** This work was supported in part by the U.S. National Science Foundation under Grant No. ECCS-1028353, by the US Air Force Office of Scientific Research under Grant No. FA9550-12-1-298; by the Presidium of the Russian Academy of Sciences under Project No. 24.31, by the Ministry of Science under Federal Research Program No. 14.V37.21.0730 and by the Siberian Division of the Russian Academy of Sciences and Siberian Federal University under Integration Project No. 101; and by the Academy of Finland and Nokia through the Center-of-Excellence program.

## References

1. A.K. Popov, Nonlinear optics of backward waves and extraordinary features of plasmonic nonlinear-optical microdevices. Eur. Phys. J. D **58**, 263–274 (2010) (topical issue on Laser Dynamics and Nonlinear Photonics)
2. A.K. Popov, V.M. Shalaev, Merging nonlinear optics and negative-index metamaterials. Proc. SPIE **8093-6**, 1–27 (2011)
3. I.V. Shadrivov, A.A. Zharov, Yu.S. Kivshar, Second-harmonic generation in nonlinear left-handed metamaterials. J. Opt. Soc. Am. B **23**, 529–534 (2006)
4. M. Scalora, G. D'Aguanno, M. Bloemer, M. Centini, N. Mattiucci, D. de Ceglia, Yu.S. Kivshar, Dynamics of short pulses and phase matched second harmonic generation in negative index materials. Opt. Express **14**, 4746–4756 (2006)
5. A.K. Popov, V.V. Slabko, V.M. Shalaev, Second harmonic generation in left-handed metamaterials. Laser Phys. Lett. **3**, 293–296 (2006)
6. A.K. Popov, V.M. Shalaev, Negative-index metamaterials: second-harmonic generation, Manley–Rowe relations and parametric amplification. Appl. Phys. B, Lasers Opt. **84**, 131–137 (2006)
7. A.K. Popov, V.M. Shalaev, Compensating losses in negative-index metamaterials by optical parametric amplification. Opt. Lett. **31**, 2169–2171 (2006)

8. A.K. Popov, S.A. Myslivets, T.F. George, V.M. Shalaev, Four-wave mixing, quantum control, and compensating losses in doped negative-index photonic metamaterials. Opt. Lett. **32**, 3044–3046 (2007)
9. A.K. Popov, S.A. Myslivets, Transformable broad-band transparency and amplification in negative-index films. Appl. Phys. Lett. **93**, 191117(3) (2008)
10. A.K. Popov, S.A. Myslivets, V.M. Shalaev, Resonant nonlinear optics of backward waves in negative-index metamaterials. Appl. Phys. B, Lasers Opt. **96**, 315–323 (2009)
11. A.K. Popov, S.A. Myslivets, V.M. Shalaev, Microscopic mirrorless negative-index optical parametric oscillator. Opt. Lett. **34**(8), 1165–1167 (2009)
12. A.K. Popov, S.A. Myslivets, V.M. Shalaev, Plasmonics: nonlinear optics, negative phase and transformable transparency (Invited Paper), in *Plasmonics: Nanoimaging, Nanofabrication, and Their Applications V*, ed. by S. Kawata, V.M. Shalaev, D.P. Tsai. Proc. of SPIE, vol. 7395, p. 73950Z-1(12) (2009)
13. A.K. Popov, S.A. Myslivets, V.M. Shalaev, Coherent nonlinear optics and quantum control in negative-index metamaterials. J. Opt. A, Pure Appl. Opt. **11**, 114028(13) (2009)
14. A.K. Popov, S.A. Myslivets, Numerical simulations of negative-index nanocomposites and backward-wave photonic microdevices, in *ICMS 2010: International Conference on Modeling and Simulation*. Proc. of WASET, vol. 37, pp. 107–121 (2010). http://www.waset.org/journals/waset/v37/v37-16.pdf
15. A.K. Popov, T.F. George, Computational studies of tailored negative-index metamaterials and microdevices, in *Computational Studies of New Materials II: From Ultrafast Processes and Nanostructures to Optoelectronics, Energy Storage and Nanomedicine*, ed. by T.F. George, D. Jelski, R.R. Letfullin, G. Zhang (World Scientific, Singapore, 2011)
16. A.I. Maimistov, I.R. Gabitov, E.V. Kazantseva, Quadratic solitons in media with negative refractive index. Opt. Spectrosc. **102**, 90–97 (2007)
17. A.I. Maimistov, I.R. Gabitov, Nonlinear optical effects in artificial materials. Eur. Phys. J. Spec. Top. **147**, 265–286 (2007)
18. S.O. Elyutin, A.I. Maimistov, I.R. Gabitov, On the third harmonic generation in a medium with negative pump wave refraction. J. Exp. Theor. Phys. **111**, 157–169 (2010)
19. L.I. Mandelstam, Group velocity in a crystal lattice. Ž. èksp. Teor. Fiz. **15**, 475–478 (1945)
20. M.I. Shalaev, S.A. Myslivets, V.V. Slabko, A.K. Popov, Negative group velocity and three-wave mixing in dielectric crystals. Opt. Lett. **36**, 3861–3863 (2011)
21. Y.R. Shen, N. Bloembergen, Theory of stimulated Brillouin and Raman scattering. Phys. Rev. **137**, A1787–A1805 (1965)
22. R.W. Boyd, *Nonlinear Optics*, 3rd edn. (Academic Press, Amsterdam, 2008)
23. D.L. Bobroff, Coupled-modes analysis of the phonon–photon parametric backward-wave oscillator. J. Appl. Phys. **36**, 1760–1769 (1965)
24. J.B. Khurgin, Mirrorless magic. Nat. Photonics **1**, 446–448 (2007)
25. V.S. Gorelik, *Contemporary Problems of Raman Spectroscopy* (Nauka Publishing Co., Moscow, 1978), pp. 28–47 (in Russian)
26. E. Anastassakis, S. Iwasa, E. Burstein, Electric-field-induced infrared absorption in diamond. Phys. Rev. Lett. **17**, 1051–1054 (1966)
27. Y. Chen, J.D. Lee, Determining material constants in micromorphic theory through phonon dispersion relations. Int. J. Eng. Sci. **41**, 871–886 (2003)
28. V.M. Agranovich, Y.R. Shen, R.H. Baughman, A.A. Zakhidov, Linear and nonlinear wave propagation in negative refraction metamaterials. Phys. Rev. B **69**, 165112 (2004)
29. V.M. Agranovich, Yu.N. Gartstein, Spatial dispersion and negative refraction of light. Phys. Uspekhi, **176**, 1051–1068 (2006) (also in *Physics of Negative Refraction*, ed. by C.M. Krowne, Y. Zhang (Springer, 2007))
30. I. Nefedov, S. Tretyakov, Ultrabroadband electromagnetically indefinite medium formed by aligned carbon nanotubes. Phys. Rev. B **84**, 113410 (2011)
31. P.A. Belov, A.A. Orlov, A.V. Chebykin, Yu.S. Kivshar, Spatial dispersion in layered metamaterials, in *Proceedings of the International Conference on Electrodynamics of Complex Materials, for Advanced Technologies, PLASMETA'11*, September 21–26, Samarkand, Uzbekistan (2011), pp. 30–31
32. I.S. Nefedov, Electromagnetic waves propagating in a periodic array of parallel metallic carbon nanotubes. Phys. Rev. B **82**, 155423(7) (2010)
33. I.S. Nefedov, S.A. Tretyakov, Effective medium model for two-dimensional periodic arrays of carbon nanotubes. Photonics Nanostruct. Fundam. Appl. **9**, 374–380 (2011) (TaCoNa-Photonics 2010)
34. P.A. Belov, R. Marques, S.I. Maslovski, I.S. Nefedov, M. Silveirinha, C.R. Simovski, S.A. Tretyakov, Strong spatial dispersion in wire media in the very large wavelength limit. Phys. Rev. B **67**, 113103 (2003)